# MOLECULAR GENETIC ANALYSIS OF THE *DILUTE-SHORT EAR* (*D-SE*) REGION OF THE MOUSE

EUGENE M. RINCHIK,*[,1] LIANE B. RUSSELL,[†] NEAL G. COPELAND*[,2] AND NANCY A. JENKINS*[,2]

** Department of Microbiology and Molecular Genetics, University of Cincinnati College of Medicine, Cincinnati, Ohio 45267-0524, and † Biology Division, Oak Ridge National Laboratory, P.O. Box Y, Oak Ridge, Tennessee 37830*

Manuscript received September 3, 1985
Accepted October 17, 1985

ABSTRACT

Genes of the *dilute-short ear* (*d-se*) region of mouse chromosome *9* comprise an array of loci important to the normal development of the animal. Over 200 spontaneous, chemically induced and radiation-induced mutations at these loci have been identified, making it one of the most genetically well-characterized regions of the mouse. Molecular analysis of this region has recently become feasible by the identification of a dilute mutation that was induced by integration of an ecotropic murine leukemia virus genome. Several unique sequence cellular DNA probes flanking this provirus have now been identified and used to investigate the organization of wild-type chromosomes and chromosomes with radiation-induced *d-se* region mutations. As expected, several of these mutations are associated with deletions, and, in general, the molecular and genetic complementation maps of these mutants are concordant. Furthermore, a deletion breakpoint fusion fragment has been identified and has been used to orient the physical map of the *d-se* region with respect to the genetic complementation map. These experiments provide important initial steps for analyzing this developmentally important region at the molecular level, as well as for studying in detail how a diverse group of mutagens acts on the mammalian germline.

SEVERAL genes that are important for normal development have been identified within the *dilute-short ear* (*d-se*) region of the mouse. The first gene to be described for the region was the recessive mutation *dilute* (*d*) (for a review, see SILVERS 1979). This is an old mutation of the mouse fancy that has a single phenotypic effect, a lightening of coat color when homozygous. This dilution of coat color is associated with a change in melanocyte morphology; wild-type melanocytes possess long, thick dendritic processes, whereas dilute melanocytes exhibit few or no processes. This morphological change results in a redistribution of melanin pigment within the melanocyte and hair shaft, but the amount of melanin synthesized remains normal (MARKERT and

[1] Present address: Biology Division, Oak Ridge National Laboratory, P. O. Box Y, Oak Ridge, Tennessee 37830.
[2] Present address: Mammalian Genetics Laboratory, LBI-Basic Research Program, NCI-Frederick Cancer Research Program, P.O. Box B, Building 539, Frederick, Maryland 21701.

SILVERS 1956; SILVERS 1979). Several other spontaneous forward mutations to *d* have subsequently been identified, but unlike the original *d* mutation, most of these alleles are associated with a severe neuromuscular disorder in homozygotes, characterized by convulsions and opisthotonus (arching upward of the head and tail), and homozygous animals usually die by about 3 weeks of age (SEARLE 1952; SILVERS 1979; RUSSELL 1971). The recessive *short-ear* (*se*) mutation arose spontaneously in mice obtained from a commercial breeder (LYNCH 1921). Homozygous *se/se* animals have short, slightly ruffled ears resulting from a defective cartilage framework. In addition, the whole skeleton is abnormal, being slightly smaller than normal with numerous other defects, including a reduced or bifurcated xiphisternum; reduced number of ribs and sternebrae; and reduction or absence of the ulnar sesamoid bone of the wrist, the medial sesamoid bone of the knee and the anterior tubercles of the sixth cervical vertebra (GREEN 1981). The *d* and *se* loci are closely linked on chromosome *9,* 0.16 centimorgans (cM) apart (GATES 1928; RUSSELL 1971).

An important step in the analysis of the *d* and *se* genes, as well as of the chromosomal region around them, was the incorporation of the *d* and *se* mutations into tester stocks employed in specific-locus mutagenesis screens (RUSSELL 1951). The specific-locus test is used to detect germinal mutations, either spontaneous or mutagen-induced, among large breeding populations of mice. Genetically uniform wild-type animals are treated with a potential mutagen and are then crossed to a multiple-recessive tester stock, homozygous for several mutations, including *a* (*non-agouti*), *b* (*brown*), $c^{ch}$ (*chinchilla*), *d* (*dilute*), *se* (*short-ear*), *p* (*pink-eyed dilution*), and *s* (*piebald spotting*). Thus, in the first-descendent generation, recessive mutations at any of these loci can be identified. Many hundreds of mutations at these loci have been recovered over the years with this technique, including several at the *d* and *se* loci.

The *d-se* region mutations that were identified among offspring of mice irradiated with neutrons, X rays or gamma rays, and among corresponding control offspring, fall into distinct classes (RUSSELL 1971). Some of the mutations ("*d*" and "*se*") are phenotypically indistinguishable from the old *d* and *se* mutations found in the tester stock, and they may represent spontaneous mutations fortuitously recovered from irradiated parents, as well as representing radiation-induced mutations. However, several other classes of mutants were noted: $d^{x}$ (*dark dilute, viable*), $d^{op}$ (*dilute-opisthotonic*), $d^{pl}$ (*dilute-prenatal-lethal*), $se^{x}$ (*intermediate ear, viable*), $se^{l}$ (*short-ear lethal*) and *Df(dse)* (*deficiency dilute short-ear*). The last two classes were not found in controls. The $d^{x}/d^{x}$ mutants are intermediate in phenotype between dilute and wild type. Similarly, the $se^{x}/se^{x}$ mutants are intermediate in phenotype between short-ear and wild type. The $d^{op}/d^{op}$ animals are dilute in color, but develop a severe neuromuscular disorder resembling opisthotonus soon after birth and usually die by 3 weeks of age. [These animals are similar in phenotype to animals homozygous for the spontaneous mutation $d^{l}$ (*dilute-lethal*) (SEARLE 1952)]. The mutations of the $d^{pl}$, $se^{l}$ and *Df(dse)* classes are all recessive lethals; embryos homozygous for these classes of mutations die before birth. The *Df(dse)* mutations were identified in animals found to be simultaneously dilute and short-eared, and

they probably represent large chromosomal deletions that remove at least the 0.16 cM region that spans the *d* and *se* loci (RUSSELL 1971). It also is interesting to note that animals of the $d^{op}/d$, $d^{pl}/d$ and *Df(dse)/d* genotypes are indistinguishable in phenotype from *d/d* animals; likewise, a $se^{t}/se$ and *Df(dse)/se* mouse cannot be distinguished phenotypically from a *se/se* mouse (RUSSELL 1971).

The genetic complexity of the *d-se* region was demonstrated by extensive complementation analyses, originally undertaken to obtain information about the chromosomal nature of mutations induced by different types of radiation treatment. The major assumption of these analyses was that the lack of complementation for a specific phenotype between any two mutations indicates that those mutants carry overlapping deficiencies covering the functional unit responsible for that phenotype. More than 800 pairwise combinations of individual mutations were analyzed for complementation of the pigment, skeletal, neurological and lethality phenotypes. Nine functional units were implicated in these analyses: five factors responsible for lethality ($l_1$–$l_5$), one factor for the dilute/melanocyte morphology phenotype (*d*), one for the neuromuscular opisthotonic phenotype (*op*), one for the short-ear phenotype (*se*) and one for another neurological disorder, Snell's waltzer (*sv*), previously mapped by linkage analysis 2 cM distal to *se* (DEOL and GREEN 1966). From these data, the mutants could be subdivided into 16 groups, most of which fitted a linear arrangement on the assumption that the order of functional units on the complementation map was centromere-$l_1$—*d*—*op*—$l_2$—$l_3$—*se*—$l_4$—*sv*—$l_5$ (RUSSELL 1971). (Since *d* and *op* had not been separable by complementation, no conclusion was possible about their order relative to each other).

The molecular analysis of the *d-se* region was initiated by the discovery that the original *d* mutation that is carried in common inbred strains of mice was associated with the site of integration of an ecotropic murine leukemia provirus (JENKINS *et al.* 1981). This ecotropic provirus, *Emv-3*, cosegregated with *d* in all inbred and recombinant inbred strains analyzed. Furthermore, in all germline phenotypic revertants of dilute ($d^{+}$) examined, reversion to wild-type coat color correlated with the loss of most of the ecotropic proviral genome (COPELAND, HUTCHISON and JENKINS 1983). Molecular cloning, restriction enzyme analysis and DNA sequencing of revertant sites have indicated that exactly one long terminal repeat (LTR) remains behind in each revertant (COPELAND, HUTCHISON and JENKINS 1983; HUTCHISON, COPELAND and JENKINS 1984). These results suggest that the provirus most likely induced the dilute mutation by integrating into noncoding regions in or around the actual dilute gene, since revertant animals are phenotypically wild type (intense in color), but still carry a viral LTR at the *d* locus. This hypothesis is supported by the fact that 600 base pairs (bp) of DNA sequence immediately surrounding the proviral integration site contain a nonsense codon on average every 50 base pairs in all six possible reading frames (HUTCHISON, COPELAND and JENKINS 1984). Thus, it is important to differentiate between the old *d* mutation, which is virally induced and is carried in many common laboratory strains of mice, and reisolates of *d*, which are new spontaneous, chemically induced or radiation-

induced mutations that do not appear to be associated with MuLV DNA sequences. For this reason, we propose to designate the virally induced dilute mutation $d^v$ to avoid confusion with other mutations.

In the experiments described here, we have isolated a series of unique-sequence cellular DNA probes from regions both 5′ and 3′ to the proviral integration site within the *d* locus. These probes have been used for deletion-mapping experiments with a variety of radiation-induced *d-se* mutations. These experiments provide a conceptual framework for a detailed molecular genetic analysis of the *d-se* region.

## MATERIALS AND METHODS

**Mice:** All mutant mice are maintained as closed-colony, noninbred stocks at the Oak Ridge National Laboratory Biology Division. The $d^v$ allele refers to the mutant allele of dilute that is virally induced. The *d-se* region mutants were identified by the specific-locus method among offspring of irradiated or control parents, and they are maintained as described (RUSSELL 1971). Briefly, the $d^{op}$ mutants (C series) are maintained by intercrossing $d^{op}$ +/$d^v$ *se* mice and selecting for dilute, nonopisthotonic segregants with long ears ($d^{op}$ +/$d^v$ *se*). In each generation, dilute short-ear segregants are discarded, and dilute opisthotonic, $d^{op}$ +/$d^{op}$ + homozygotes are selected for DNA analysis. The $d^{pl}$ mutants (A series) are maintained by crossing $d^{pl}$ +/+ *se* to $d^{op}$ +/$d^v$ *se*. Dilute segregants with long ears ($d^{pl}$ +/$d^v$ *se*) are then crossed to $d^{op}$ +/+ *se* to regenerate the $d^{pl}$ +/+ *se* nondilute, long-ear type. The *Df(dse)* mutants (B series) are maintained by alternate crosses to $d^v$ +/$d^v$ + and + *se*/+ *se*, selecting for dilute and short-ear progeny, respectively. The $se^l$ mutants (D series) are maintained by intercrossing + $se^l$/$d^v$ + animals selecting for nondilute segregants with long ears (+ $se^l$/$d^v$ +) in each generation. The + $se^l$/+ $se^l$ segregants die *in utero*, and the $d^v$ +/$d^v$ + dilute segregants are discarded. For genomic DNA analysis, mutants of the B and D classes, with the exception of Bb2, were balanced opposite a $d^v$ + chromosome; mutants of the A class were balanced opposite $d^v$ *se*. The C57BL/6J and DBA/2J inbred strains were obtained from the Jackson Laboratory, Bar Harbor, Maine.

**Hybridization probes and phage library screens:** The p0.3 probe (see RESULTS), previously designated the Pst probe, contains 4.5 kb of pBR325 and the 2.6-kb *Pst*I-*Eco*RI fragment of unique cellular DNA from the 3′ end of λ·Emv-3 (COPELAND, HUTCHISON and JENKINS 1983). The p0.3 probe was used to screen a partial *Sau*3A library from the DBA/2J strain in λEMBL3 (kindly provided by H. LEHRACH), using the plaque-lift method of BENTON and DAVIS (1977). A single positive plaque was identified and replated, and phage DNA was isolated. A 1.1-kb *Hin*dIII-*Sal*I fragment from the 3′ end of the DBA/2-derived phage λDSE-RI (D) was subcloned into pBR325 to generate the probe designated pR1.3. The *Sal*I terminus of this insert was derived from the polylinker in the EMBL3 cloning vector.

A 1.3-kb *Pvu*II fragment from the 5′ end of the Emv-3 clone (COPELAND, HUTCHISON and JENKINS 1983) was blunt-end ligated to *Pvu*II-digested pBR329 to generate a probe designated p0.5. This probe, however, contained a moderately repetitive sequence that detected multiple bands in Southern analysis of genomic DNA. A 200-bp fragment of the 1.3-kb insert was generated by digestion with *Alu*I and was blunt-end ligated to *Sma*I-digested pUC8 to generate the probe p0.7. The derivation of probe p94.1 is described below.

**DNA isolation, restriction enzyme analysis, DNA transfers and hybridization:** High-molecular-weight DNA was prepared as described in JENKINS *et al.* (1982). The DNA (5 μg/lane) was digested to completion with an excess of restriction enzyme (Bethesda Research Laboratories; New England Biolabs). Digested DNAs were electrophoresed through 0.8% agarose and were transferred to the nylon membrane Zeta-Por (AMF-CUNO) in 10 × SSC. Filters were then baked 1 hr at 80° under vacuum, washed

for 1 hr at 65° in 0.1 × SSC, 1% SDS, prehybridized for 2 hr at 65° in 4 × SSCP, 1% SDS, 1 × Denhardts and hybridized for 18–20 hr at 65° with $^{32}$P-labeled nick-translated probe (>2 × $10^8$ cpm/$\mu$g) in 4 × SSCP, 1% SDS, 1 × Denhardts and 10% sodium dextran sulfate. Filters were washed at 65° (stringent wash was 0.1 × SSC, 0.2% SDS for 30 min at 65°), air dried, and autoradiographed at −70°, using Kodak XAR-5 X-ray film and DuPont Lightning-Plus intensifying screens.

**Cloning of cellular DNA from the Aa2 ($d^{pl}$) mutant:** To clone the aberrant 3.3-kb *Eco*RI fragment (ΔfAa2) detected by the p0.3 probe in Southern analysis of genomic DNA of the Aa2 $d^{pl}$ mutant, spleen DNA from an animal of the genotype Aa2 $d^{pl}$ +/ $d^{v}$ *se* was digested to completion with an excess of *Eco*RI, and fragments of 2.5–4.5 kb in length were enriched by electrophoresis through low-melting agarose. These fragments were eluted from the agarose, phenol- and chloroform-extracted and passed once through a NACS-Prepac Column (Bethesda Research Laboratories) according to instructions provided by the manufacturer. These size-selected fragments then were ligated to *Eco*RI arms of λgtWes·λB and packaged *in vitro*, and recombinant phage were screened with the p0.3 probe. Positive plaques were replated, and phage DNAs were isolated. The 3.3-kb *Eco*RI insert was then subcloned into pBR325 for restriction analysis. A 0.5-kb *Eco*RI-*Hin*dIII fragment of this insert subsequently was subcloned into pBR325 to generate the p94.1 probe.

**Densitometry analysis:** The hydridization intensity of specific fragments of genomic DNA after Southern analysis was used to determine genomic copy number of the probe sequence employed in the hybridization. Genomic DNA from the *d-se* region mutants was digested with *Eco*RI, transferred to Zeta-Por following electrophoresis and probed with a mixture of the clones p94.1 and p15.4a. The 1.0-kb *Eco*RI fragment detected by the p15.4a probe (see RESULTS) served as a reference band to standardize the amount of DNA loaded into each lane. The hybridization profiles from autoradiograms were scanned with a densitometer, and the resultant plots of hybridization intensity were integrated using arbitrary units. The ratio of the integrated value for the p94.1 band divided by the valued for the standard p15.4a band for experimental samples was compared to that same ratio obtained from various homozygous (two copy) control DNAs to obtain estimates of copy number for each mutant.

## RESULTS

**Current complementation map of the *d-se* region:** The complementation map of the *d-se* region published by RUSSELL (1971) has been refined by the analysis of greater numbers of crosses and addition of mutants. Additional lethal factors have been identified, both of the prenatal (*pl*) and neonatal (*nl*) types. Figure 1 represents the current proposed *d-se* complementation map for that subset of radiation-induced mutations that was analyzed in the experiments described here. The existence of neonatal lethal factors has been hypothesized to explain why certain crosses between mutants produce a higher than expected frequency of offspring dying before classification and/or a deficit in certain classes of offspring (L. B. RUSSELL, unpublished observations). Loss of these proposed *nl* functional units may result in decreased fitness of the neonate, a situation similar to that described for a site near the *albino* (*c*) locus that is important for juvenile survival (RUSSELL and DEHAMER 1973; RUSSELL, MONTGOMERY and RAYMER 1982). Because, to date, none of the dilute radiation-induced mutants shown in Figure 1 have complemented one another for the dilute or opisthotonic phenotypes, the *d* and *op* functions are shown at the same site. The complementation map is drawn linearly with the order cen-

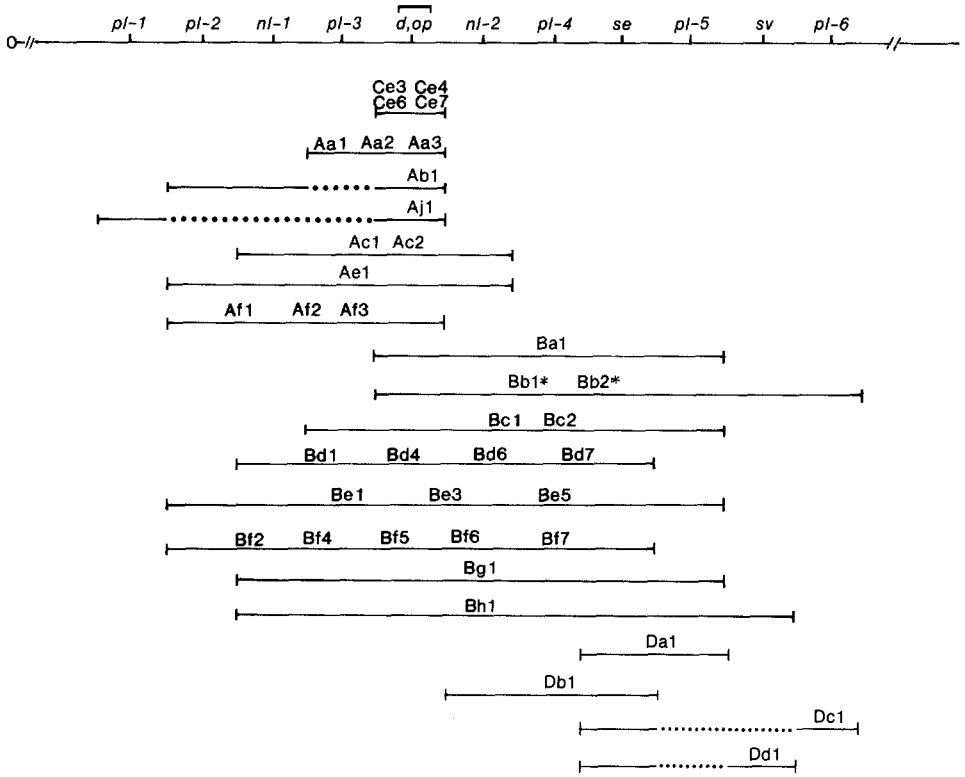


FIGURE 1.—Complementation map of the *d-se* region. Four classes of *d-se* region mutations from radiation experiments have been analyzed in these studies. These include $d^{pl}$, *Df(dse)*, $d^{op}$ and $se^{l}$, which are referred to as group A, B, C and D mutants, respectively. Members of the same complementation group are indicated by the same second letter designation, and individual members of a complementation group are identified by a numerical designation. Horizontal bars represent the extent of the presumed deficiency for mutants in each complementation group. The complementation map is drawn linearly, with the centromere at the left (indicated by 0); no correlation with physical distance is implied. Functional units include *pl-1* through *pl-6, prenatal lethals*; *nl-1* and *nl-2, neonatal lethals*; *d, dilute*; *op, opisthotonus*; *se, short-ear*; and *sv, Snell's waltzer*. Since *d* and *op* have not, to date, been separable by complementation, they are shown at the same site. "Skipping" mutations are indicated by dotted lines, and mutations that behave aberrantly in complementation tests are indicated by an asterisk (see text for further explanation).

tromere-*pl-1—pl-2—nl-1—pl-3—d,op—nl-2—pl-4—se—pl-5—sv—pl-6*. No correlation with physical distance is implied.

Four classes of *d-se* region mutations from radiation experiments have been analyzed in these studies. These include $d^{pl}$, *Df(dse)*, $d^{op}$ and $se^{l}$. These mutants will subsequently be referred to as group A, B, C and D mutants, respectively. Members of the same complementation group are indicated by the same second-letter designation, and individual members of a complementation group are identified by a numerical designation. For example, Aa1, Aa2 and Aa3 are all members of a single $d^{pl}$ complementation group (Figure 1). Previously published mutant designations are listed in Table 1. Solid lines ending in vertical bars represent the extent of the presumed deficiency in any comple-

TABLE 1

**Summary of the deletions detected in radiation-induced *d-se* region mutations**

| Mutant designation[a] | Mutant class | *Kpn*I-fragment size (kb)[b] | Deletion detectable with probe p0.3[c] | Deletion detectable with probe p94.1[d] |
|---|---|---|---|---|
| Aa1 (7G) | $d^{pl}$ | 9.2, 25 | No | No |
| Aa2 (19R145H) | $d^{pl}$ | 9.2, 5.4 | Yes | Yes |
| Aa3 (19DThWb) | $d^{pl}$ | 9.2, 25 | No | Yes |
| Ab1 (1d[l]) | $d^{pl}$ | 9.2, 25 | No | No |
| Aj1 (15DTD) | $d^{pl}$ | 9.2, 25 | No | No |
| Ac1 (3FAFyc) | $d^{pl}$ | 9.2 | Yes | Yes |
| Ac2 (19Zb) | $d^{pl}$ | 9.2 | Yes | Yes |
| Ae1 (9R250M) | $d^{pl}$ | 9.2 | Yes | Yes |
| Af1 (3FrS) | $d^{pl}$ | 9.2 | Yes | Yes |
| Af2 (21R75M) | $d^{pl}$ | 9.2, 25 | No | Yes |
| Af3 (3FR60Hc) | $d^{pl}$ | 9.2 | Yes | Yes |
| Ba1 (11R145L) | *Df (dse)* | 9.2 | Yes | No |
| Bb1 (1R75H) | *Df (dse)* | 9.2 | Yes | No |
| Bb2 (3R75H) | *Df (dse)* | 9.2 | ND[e] | Yes |
| Bc1 (13R60L) | *Df (dse)* | 9.2 | Yes | Yes |
| Bc2 (1R145H) | *Df (dse)* | 9.2 | Yes | No |
| Bd1 (39FATw) | *Df (dse)* | 9.2 | Yes | Yes |
| Bd4 (94FBFo) | *Df (dse)* | 9.2 | Yes | Yes |
| Bd6 (8FR60L) | *Df (dse)* | 9.2 | Yes | Yes |
| Bd7 (1DTD) | *Df (dse)* | 9.2 | Yes | Yes |
| Be1 (4DTD) | *Df (dse)* | 9.2 | Yes | Yes |
| Be3 (11FHAFo) | *Df (dse)* | 9.2 | Yes | Yes |
| Be5 (13SaSd) | *Df (dse)* | 9.2 | Yes | Yes |
| Bf2 (37FBFo) | *Df (dse)* | 9.2 | Yes | Yes |
| Bf4 (17Zb) | *Df (dse)* | 9.2 | Yes | Yes |
| Bf5 (18FATw) | *Df (dse)* | 9.2 | Yes | Yes |
| Bf6 (23YPSa) | *Df (dse)* | 9.2 | Yes | Yes |
| Bf7 (10FDFoD) | *Df (dse)* | 9.2 | Yes | Yes |
| Bg1 (2R250M) | *Df (dse)* | 9.2 | Yes | Yes |
| Bh1 (209G) | *Df (dse)* | 9.2 | Yes | Yes |
| Ce3 (11FrTh) | $d^{op}$ | 25 | No | No |
| Ce4 (3UThb) | $d^{op}$ | 25 | No | No |
| Ce6 (40K) | $d^{op}$ | 25 | No | No |
| Ce7 (55K) | $d^{op}$ | 25 | No | No |
| Da1 (5RD300H) | $se^{l}$ | 9.2, 25 | No | ND |
| Db1 (52CoS) | $se^{l}$ | 9.2, 25 | No | No |
| Dc1 (32DTD) | $se^{l}$ | 9.2, 25 | No | ND |
| Dd1 (10R250H) | $se^{l}$ | 9.2, 25 | No | ND |

[a] Mutant designations are as described in Figure 1. Previously published designations are given in parentheses for reference.

[b] *Kpn*I restriction enzyme fragments were identified as described in Figure 3. All mutant chromosomes were balanced over $d^{v}$-containing chromosomes, as diagrammed in Figure 3, with the exception of $d^{op}$ mutants that were homozygous $d^{op}$. A 9.2-kb *Kpn*I fragment is obtained from the balancer $d^{v}$-containing chromosome (Figure 2). A 25-kb fragment is indicative of a chromosome that is wild type in the region analyzed.

[c] Loss of a 25-kb *Kpn*I fragment suggests the presence of a chromosome deleted in the region defined by probe p0.3.

[d] Deletions in the region defined by probe p94.1 were assigned by hybridization intensity. Each DNA sample was analyzed an average of three times, and in all cases, unambiguous typing was possible. The results were confirmed for the Ab1, Aj1, Ba1, and Db1 mutants (Figure 6).

[e] Mutant Bb2 was not available in combination with a balancer $d^{v}$ *se* or $d^{v}$ + chromosome. Mutant Bb2 is now extinct and not available for further analysis. ND = not determined.

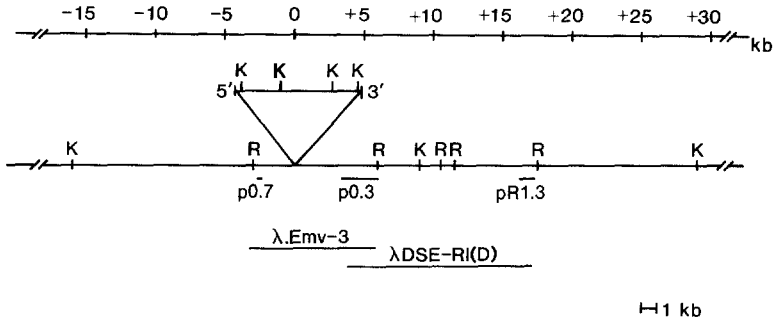


FIGURE 2.—Limited genomic restriction map of the *Emv-3* integration site. The *Emv-3* integration site has been assigned position zero. The direction of *Emv-3* transcription is indicated. Distances in kilobases (kb) from the site of virus integration are denoted by minus and plus numbers. The origins of the probe sequences p0.7, p0.3 and pR1.3, as well as the overlapping λ clones, are described in the text. K, *Kpn*I; R, *Eco*RI.

mentation group. Areas of overlap between any two complementation groups were inferred from the failure of mutants from different groups to complement for a specific phenotype.

Two unusual $d^{pl}$ mutations, Ab1 and Aj1, are included in Figure 1. These can be fitted into a linear map only by being designated as "skipping" mutations; Aj1 appears to "skip" *pl-2, nl-1* and *pl-3,* whereas Ab1 "skips" *pl-3.* The regions "skipped" over in these mutants are indicated by a dotted line in Figure 1. Each of two $se^{l}$ "skipping" mutations, Dc1 and Dd1, was earlier shown not to have resulted from independent, recombinationally separable lesions (RUSSELL 1971). Other unusual mutations are represented by Bb1 and Bb2. Bb1 is prenatally lethal in combination with Ac2 or Ae1, and Bb2 is lethal with Aa1 or Ae1; but neither Bb1 nor Bb2 is lethal with any other A-group mutation that extends through *pl-3* (L. B. RUSSELL, unpublished results). The aberrant complementation of these two mutations, which cannot be explained at present, is signified by an asterisk in Figure 1.

**Limited genomic restriction map around the proviral integration site at *d*:** Previously, we obtained a λ clone of *Eco*RI-digested DBA/2J ($d^{v}/d^{v}$) DNA that contained the entire ecotropic provirus associated with $d^{v}$, as well as approximately 9 kb of flanking cellular DNA (COPELAND, HUTCHISON and JENKINS 1983). This clone is designated λ·Emv-3 in Figure 2. Subsequently, a unique 2.6-kb *Pst*I-*Eco*RI fragment of cellular DNA from the extreme 3′ end of λ·Emv-3 was identified and subcloned into plasmid pBR325 (COPELAND, HUTCHISON and JENKINS 1983). This subclone is designated p0.3 in Figure 2. Likewise, a 0.2-kb fragment of cellular DNA from the 5′ end of λ·Emv-3 has been identified and subcloned in pUC8 (see MATERIALS AND METHODS). This subclone has been designated p0.7 (Figure 2). Finally, by screening a λ library of DBA/2J liver DNA with p0.3, we obtained a second λ clone, λDSE-RI (D), which extends approximately 10 kb 3′ of p0.3. A unique 1.1 kb *Hind*III-*Sal*I fragment from the 3′ end of λDSE-RI (D) was subcloned in pBR325 and designated pR1.3 (Figure 2; MATERIALS AND METHODS).

The clones p0.7, p0.3 and pR1.3 were used as probes for Southern analysis

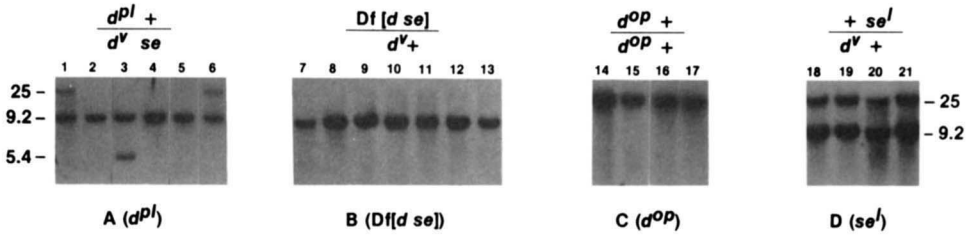


FIGURE 3.—Representative Southern analysis of genomic DNAs of *d-se* region mutations. DNAs (5 μg/lane) from animals of the indicated genotypes were digested with *Kpn*I and probed with p0.3 The classification of mutants into A, B, C and D series is presented below each blot. Fragment sizes are indicated in kilobases. Mutants analyzed include Aa1, Ae1, Aa2, Ac2, Af1, Af2, Ba1, Bb1, Bc1, Bc2, Bd4, Bd6, Bd7, Ce6, Ce7, Ce3, Ce4, Da1, Db1, Dc1 and Dd1—lanes 1–21, respectively.

of genomic DNAs isolated from C57BL/6J mice that are wild type at *d* (+/+) or from DBA/2J mice homozygous for $d^{v}$. A limited *Eco*RI and *Kpn*I restriction-enzyme map for approximately 45 kb of cellular DNA flanking *Emv-3* is shown in Figure 2. In this map, the site of virus integration is considered position zero. Distances in kilobases (kb) from the site of provirus integration are indicated by minus and plus numbers signifying 5′ and 3′ directions, respectively, in relation to the direction of viral RNA transcription. The *Eco*RI and *Kpn*I sites from −3 to +18 were determined by restriction analysis of λ·Emv-3 and λDSE-RI (D). The *Kpn*I sites at positions −16 and +29 were determined by Southern analysis of genomic DNAs hybridized with p0.7 and pR1.3, respectively. *Eco*RI sites between −3 to −16 and between +18 to +29 could not be determined in these experiments. In total, approximately 45 kb of cellular DNA flanking *Emv-3* can be screened for deletions, insertions or rearrangements in mutant *d-se* chromosomes by *Kpn*I digestion of genomic DNA and hybridization with the p0.3 and pR1.3 probes (Figure 2).

**Structural confirmation of the deletional nature of many of the radiation-induced *d-se* region mutations:** To determine if sequences from −16 to +29 were deleted in radiation-induced $d^{op}$, $d^{pl}$, $se^{l}$ and *Df* (*dse*) mutations, we analyzed DNAs from mice carrying 38 different *d-se* region mutations (Figure 1; Table 1). Initially, DNAs were digested with *Kpn*I and were hybridized with the p0.3 probe. Representative results are shown in Figure 3, and a summary of all the data is given in Table 1. A 25-kb *Kpn*I fragment is representative of a wild-type chromosome (Figure 2). An aberrantly sized fragment might indicate a fragment carrying a deletion, insertion or rearrangement. The complete absence of a fragment would be expected for a deletion covering the sequences included in the hybridization probe.

In the case of $d^{op}$ mutants, it was possible to analyze DNA from $d^{op}/d^{op}$ homozygotes, because these mice do not die until 3 weeks of age. However, this was not possible with $d^{pl}$, $se^{l}$ or *Df* (*dse*) mice, because these mutations are all prenatal lethals. This complicates the detection of deletions, since one wild-type chromosome typically would be present in stocks carrying each of these mutations, and therefore, if the mutant chromosome carried a large deletion (including the region corresponding to p0.3), it could only be detected by

differences in hybridization intensity. To overcome this problem, all $d^{pl}$, $se^{l}$ and *Df(dse)* chromosomes were balanced over a $d^{v}$ *se*, or $d^{v}$ + chromosome. These constructions mark the balancer chromosome with *Emv-3*, generating a 9.2-kb *Kpn*I fragment following hybridization with p0.3 (Figure 2). Therefore, it was possible to directly screen for deletions in these mutant chromosomes. The *se* mutation present in several cases on the balancer chromosome represents the original spontaneous *se* mutation that was used to mark genetically the balancer chromosome. Mice carrying this mutation are wild type within the region −16 and +29 kb (data not shown), so that the presence of this mutation does not complicate the interpretation of the results that follow.

All four of the $d^{op}/d^{op}$ DNAs analyzed (Figure 3; Table 1) generated wild-type 25-kb *Kpn*I fragments following hybridization with p0.3, suggesting either (1) that these mutations lie outside of the 25-kb region detected with p0.3 or (2) that they are induced by single base changes or by deletions or insertions that are too small to be detected by this analysis.

In contrast, all *Df(dse)* mutations analyzed were deleted for sequences hybridizing to p0.3, because no 25-kb *Kpn*I fragments were detected. This was expected, because these mutations were thought to represent large deletions covering both *d* and *se*. However, the molecular analysis provides the first formal proof that these were, indeed, deletions.

In the case of the $d^{pl}$ mutations, some mutations were deleted for sequences homologous to p0.3 and some were not. This was consistent with the $d^{pl}$ mutations being deficiencies intermediate in size between $d^{op}$ and *Df(dse)* (Figure 1). In the case of $d^{pl}$ mutant Aa2, an aberrantly sized 5.4-kb *Kpn*I fragment was detected (Figure 3, lane 3) in addition to the 9.2-kb *Kpn*I fragment representing the balancer chromosome, suggesting that the former may represent a deletion breakpoint fusion fragment. Further restriction analysis, as well as hybridization with p0.7, confirmed this interpretation and indicated that the deletion extends 5′ (in the minus direction) from p0.3 (data not shown).

Finally, all four $se^{l}$ mutants analyzed gave normal 25-kb *Kpn*I fragments. This result also was expected, because these mutations do to include *d*, and *se* maps 0.16 cM distal to *d*.

All of the results, summarized in Table 1, were confirmed by *Eco*RI digestion and hybridization with p0.3, and in every case the results were consistent (data not shown). In addition, all of the mutant DNAs were digested with *Kpn*I and hybridized with p0.7 or pR1.3 (data not shown). No aberrantly sized fragments were detected, suggesting that the deletions identified with p0.3 (Table 1), with the exception of $d^{pl}$ mutant Aa2, spanned the entire 45-kb region (−16 to +29) flanking *Emv-3*. Furthermore, no new deletion breakpoint fusion fragments were detected with these probes, suggesting that mutant chromosomes appearing wild type following *Kpn*I digestion and hybridization with p0.3 had not suffered large deletions, insertions or rearrangements in the entire 45 kb of cellular DNA flanking *Emv-3*.

**Molecular cloning of the deletion breakpoint fusion fragment of $d^{pl}$ mutant Aa2:** Molecular cloning of deletion breakpoint fusion fragments and identification of unique sequence hybridization probes from both sides of the dele-

tion makes it possible to obtain probes that "jump" over the deleted segment, which in some cases may represent very large distances. For example, by identifying a deletion breakpoint fusion fragment that has one end in *d* and the other in *se*, it may be possible to use probes homologous to *d*-locus sequences to "jump" into *se* without the time-consuming process of walking 0.16 cM (200–300 kb) from *d* to *se*. Once in the *se* region, it should be possible to use the various *se* radiation-induced (presumably deletion) mutations to identify the *se* gene.

The 3.3-kb *Eco*RI deletion breakpoint fusion fragment identified in mutant Aa2 spleen DNA with probe p0.3 was cloned into the *Eco*RI site of λgtWes·λB and subsequently subcloned into the *Eco*RI site of pBR325. This subclone has been designated pΔfAa2. A restriction map of the 3.3-kb pΔfAa2 *Eco*RI insert is shown in Figure 4b.

Comparison of the restriction enzyme map of the pΔfAa2 insert (Figure 4b) with that of the 3′ end of λ·Emv-3 (Figure 4a) indicates that the deletion breakpoint in mutant Aa2 is located within the 2.6-kb *Pst*I-*Eco*RI p0.3 sequence. One end of the pΔfAa2 insert matches the 3′ end of the p0.3 insert, but lacks the *Pst*I site that defines the 5′ end of p0.3. The other end of the pΔfAa2 insert is quite unlike the region normally 5′ of p0.3, confirming that this fragment represents a deletion breakpoint fusion fragment and that the deletion extends 5′ from p0.3, past both the *Emv-3* integration site and p0.7 (Figure 2). The exact size of the deletion is still unknown.

To characterize the organization of DNA located 5′ to the Aa2 deletion, as well as the corresponding region in wild-type chromosomes, we identified and subcloned a unique 0.5-kb *Eco*RI-*Hin*dIII fragment (shaded box in Figure 4b) into pBR325 and used this probe, designated p94.1, for Southern analysis of both mutant Aa2 and wild-type DNA. A limited restriction enzyme map for the region 3′ to p94.1 in wild-type chromosomes is shown in Figure 4c. Comparison of this restriction map with that of the pΔfAa2 insert (Figure 4b) suggests that the 5′ breakpoint of mutant Aa2 is localized within the 700 bp *Kpn*I-*Eco*RI fragment immediately 3′ of p94.1.

**The p94.1 probe identifies differences in the extent of many *d-se* region deletions:** The preceding results suggest that probe p94.1 marks a region of DNA 5′ to the *Emv-3* integration site. Because the deleted segment in the Aa2 mutant could be very large, and since p94.1 may be located in a region considerably 5′ to *d*, it was of interest to determine whether this region was deleted in any of the *d-se* region mutants. However, testing for a deletion within this region was difficult, especially for the $d^{pl}$, $se^{l}$ and *Df* (*dse*) mutations, both because homozygotes could not be tested directly and because a marked balancer chromosome was not available for most of the mutations to be analyzed. Therefore, deletions could only be identified by reduced hybridization intensity of probe p94.1 in mutant (presumably deleted) *vs.* wild-type DNA. As an internal standard we included a unique sequence probe, p15.4a, derived from the region immediately flanking the *Emv-15* provirus that is associated with the $A^{y}$ mutation at the agouti locus on chromosome 2 (COPELAND, JENKINS and LEE 1983). The p15.4a probe, which should be present at two copies per

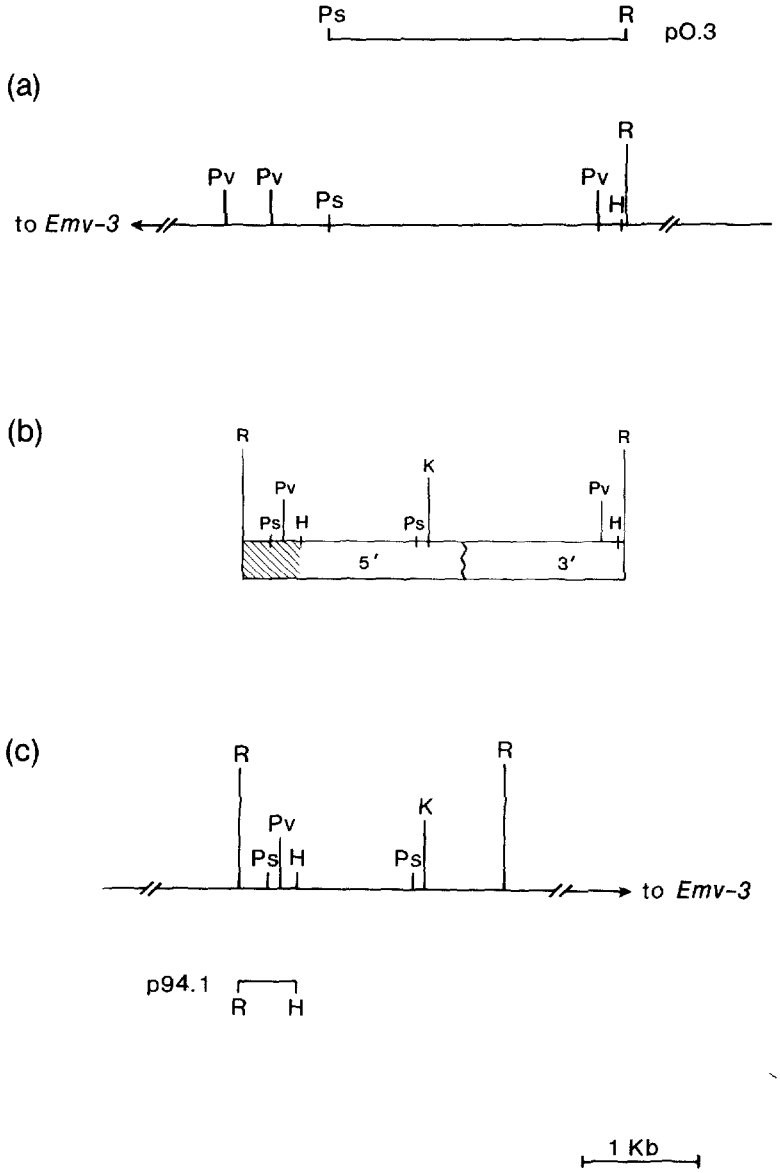


FIGURE 4.—Comparison of the restriction maps of both ends of the Aa2 $d^{pl}$ deficiency. Ps, *Pst*I; R, *Eco*RI; Pv, *Pvu*II; H, *Hin*dIII; K, *Kpn*I. (a) A map of the 3′ end of the 18-kb *Eco*RI fragment containing the *Emv-3* provirus from DBA/2J mice (COPELAND, HUTCHISON and JENKINS 1983). The p0.3 sequence is indicated. (b) Restriction map of the 3.3-kb ΔfAa2 *Eco*RI fragment. Note the similarity of the 3′ end of ΔfAa2 to the 3′ end of the fragment presented in (a). The shaded box represents the 0.5-kb *Eco*RI-*Hin*dIII p94.1 fragment (see below). The 3′ end of the ΔfAa2 fragment, defined by hybridization to the p0.3 probe and by similarities with the 3′ end of the 18-kb *Eco*RI fragment, is indicated. (c) Representative restriction map of the genomic DNA near the 5′ Aa2 $d^{pl}$ deletion breakpoint in wild-type chromosomes. Note that the $d^{pl}$ deletion breakpoint [jagged line in (b)] can be localized to a 0.7-kb *Kpn*I-*Eco*RI fragment.

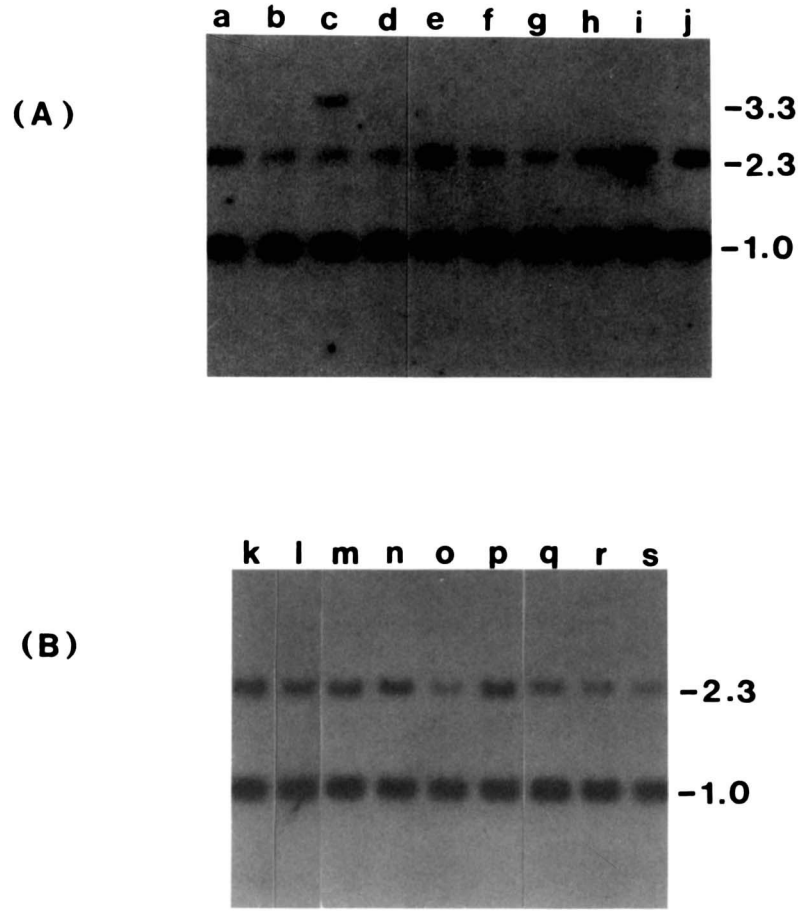


FIGURE 5.—Probe p94.1 identifies differences in the extent of many *d-se* region mutations. DNAs (5 μg/lane) from various mutants were digested with *Eco*RI and hybridized with a mixture of probes p94.1 and p15.4a. The 1.0-kb band (detected with probe p15.4a) reflects a sequence not linked to *d-se* and was used to standardize the amount of DNA loaded into each lane. Panel (A): Analysis of some A ($d^{pl}$) mutants. Lanes a, Aa1; b, Ae1; c, Aa2; d, Ac2; e, 6RC, a homozygous control; f, Aa3; g, Af1; h, Af2; i, Af3; j, Ab1. Panel (B): Analysis of some B [*Df(dse)*] mutants. Lanes k, $d^{v}$ +/$d^{v}$ + homozygous control; l, + *se*/+ *se* homozygous control; m, Ba1; n, Bb1; o, Bc1; p, Bc2; q Bd6; r, Bd7; s, Be1. Note the differences in intensity among the 2.3-kb fragments (detected with probe p94.1). The 3.3-kb *Eco*RI fragment in lane C represents the deletion breakpoint fusion fragment of $d^{pl}$ mutant Aa2.

cell in all *d-se* mutants, identifies a 1.0-kb *Eco*RI fragment in genomic DNA (N. G. COPELAND and N. A. JENKINS, unpublished results). This probe was useful for identifying intensity differences that were due to varying amounts of DNA loaded in each lane.

DNAs from the various *d-se* mutants were digested with *Eco*RI and probed with a mixture of p94.1 and p15.4a. Two representative blots from this series of experiments are shown in Figure 5. Clearly, some mutants gave a stronger hybridization signal than others with p94.1 (the 2.3-kb band), whereas the

p15.4a probe (1.0-kb band) hybridized to approximately the same degree in all mutants analyzed. Densitometry tracings confirmed that some mutants possessed only one copy of the p94.1 sequence, whereas others appeared to possess two copies. These experiments were repeated several times, and the results are summarized in Table 1.

In only one case (Figure 5, lane c) did we detect an aberrantly sized *Eco*RI fragment with probe p94.1. This result was expected, because this lane represented mutant Aa2 DNA from which p94.1 was derived. Digestion with *Kpn*I and hybridization with p94.1, which generates a 15-kb fragment, again failed to detect any abnormally size fragments (data not shown). Therefore, no deletion breakpoints other than the one carried by mutant Aa2 were detected in the 15-kb region immediately flanking p94.1 in any of the mutants analyzed.

In some cases, it was possible to confirm directly by genetic analysis the densitometry predictions of p94.1 copy number summarized in Table 1. The Aa2 $d^{pl}$ chromosome can be readily distinguished from other mutant chromosomes, because an aberrant 3.3-kb *Eco*RI fragment is detected following hybridization with p94.1. Therefore, deletion of the p94.1 sequence in other deficiencies could easily be ascertained by testing for the presence or absence of the normal 2.3-kb *Eco*RI fragment, in addition to the aberrant 3.3-kb *Eco*RI fragment, in genomic DNA from $F_1$ hybrids that carried the mutation in question opposite an Aa2 $d^{pl}$ balancer chromosome. However, this experiment could be performed only with mutants Ab1, Aj1, Ba1, Bb1 and Bb2, since these are the only $d^{pl}$ and *Df(dse)* mutations analyzed that complement the *pl-3* lethal factor associated with mutant Aa2 (see Figure 1). Therefore, Aa2 mice ($d^{pl}$ +/+ *se*) were crossed to Ab1 ($d^{pl}$ +/+ *se*), Aj1 ($d^{pl}$ +/$d^{v}$ *se*) and Ba1 [*Df(dse)*/+ *se*] mice, and dilute, opisthotonic segregants with long ears [$d^{pl}$ +/$d^{pl}$ + and *Df(dse)*/$d^{pl}$ +] were selected. Unfortunately, the Bb1 and Bb2 mutants were not available for this analysis. In addition, Aa2 ($d^{pl}$ +/$d^{v}$ *se*) was crossed to Db1 (+ $se^{l}$/$d^{v}$ +) and wild-type segregants (+ $se^{l}$/$d^{pl}$ +) were analyzed. A summary of all classes of progeny expected from the Aa2 × Ba1 cross, shown as an example, plus the results of *Eco*RI digestion of spleen DNA from the appropriate hybrids followed by probing with p94.1, is presented in Figure 6. As predicted, the Ab1, Aj1, Ba1 and Db1 chromosomes were not deleted for the p94.1 sequence, because a 2.3-kb *Eco*RI fragment was detected in all DNAs in addition to the 3.3-kb fragment derived from the Aa2 balancer chromosome. Thus, these results confirm the densitometry data which indicate that these mutants carry two copies of the p94.1 sequence.

**Correlation of the *d-se* complementation map with the physical map:** The probes p0.3 and p94.1 have been useful in determining the extent of the *d-se* region deletions. These physical data, albeit limited, now permit the orientation of the genetic complementation and physical maps with respect to one another. The data also allow for the placement of cloned DNA sequences amid complementation groups and for the discrimination among members of a specific complementation group based on the extent of their respective deletions.

For example, the Aa2 $d^{pl}$ mutant chromosome is believed to be deficient for both *d* and *op*, as well as for *pl-3*, a prenatal lethal factor immediately proximal

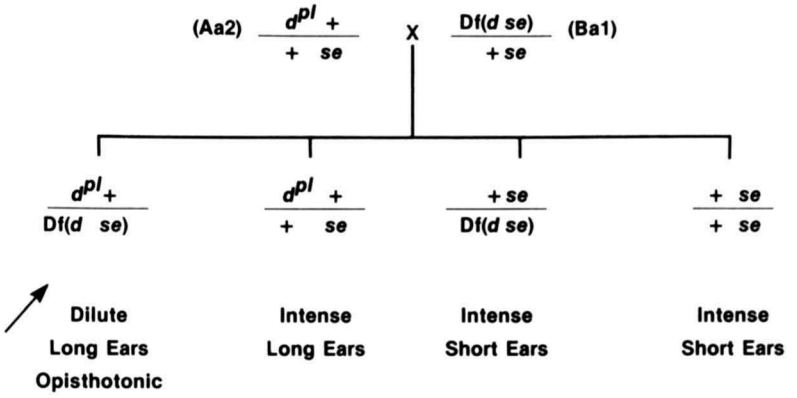


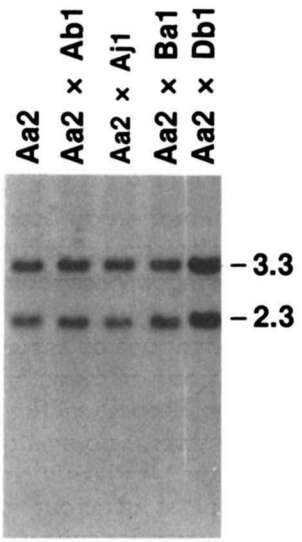


FIGURE 6.—Genetic confirmation of the presence of the p94.1 sequence in four *d-se* region mutations. A cross with expected phenotypes, used to balance the Ba1 deficiency over the Aa2 $d^{pl}$ deficiency is indicated. The arrowhead shows the class of progeny selected for analysis. Similarly, Ab1, Aj1 and Db1 were balanced over Aa2. DNAs from each specific complementing construction were digested with *Eco*RI and probed with the p94.1 sequence. Lanes, from left to right: Aa2 ($d^{pl}$ $+/d^{v}$ *se*); Aa2 × Ab1 ($d^{pl}$ $+/d^{pl}$ +); Aa2 × Aj1 ($d^{pl}$ $+/d^{pl}$ +); Aa2 × Ba1 [$d^{pl}$ $+/Df(dse)$]; Aa2 × Db1 ($d^{pl}$ +/+ $se^{l}$). Fragments sizes are indicated in kilobases.

to *d* (see Figure 1). The p0.3 probe, which is derived from a region of unique sequence cellular DNA approximately 3 kb 3′ to the *Emv-3* provirus, identifies the 3′ end of the Aa2 deletion. This result indicates that either the segment recognized by the p0.3 probe is distal to *d*, between (*d, op*) and *nl-2*, or is proximal to *d*, between *nl-1* and *pl-3*. Note that, in the former case, *Emv-3* transcription would be left to right on the complementation map, whereas in the latter case, transcription would be right to left. The pattern of absence or

presence of the p94.1 sequence, which is derived from the 5′ end of the Aa2 deletion, across the panel of *d-se* region deficiencies, and, in particular, the results for the Ba1 *Df(dse)* mutant suggest that the p94.1 probe lies between *nl-1* and *pl-3*, thereby placing the p0.3 probe between (*d, op*) and *nl-2*. This orients the 3′ end of *Emv-3* toward *se*, distal to *d*. The Ba1 *Df(dse)* deficiency includes both *d* and *se* (and presumably all DNA between *d* and *se*), but not *pl-3*. Moreover, the Ba1 chromosome is not deleted for the p94.1 sequence (see Table 1) that was confirmed by genetic analysis (Figure 6). One would expect that, if the p94.1 sequence, which recognizes the 5′ end of the Aa2 deficiency, were between (*d, op*) and *nl-2*, it would be deleted in the Ba1 chromosome. Likewise, the $d^{pl}$ mutant Af2, which deletes *pl-2, nl-1, pl-3,* (*d, op*) and the p94.1 sequence, but not the p0.3 sequence, suggests that p94.1 is proximal to (*d, op*), whereas p0.3 is distal to (*d, op*).

Figure 7 depicts a composite map of the *d-se* region, reflecting the placement of the DNA probes p94.1 (with its associated 15 kb of genomic DNA) and p0.7/p0.3/pR1.3 (with their associated 45 kb) onto the complementation map. This map position of the p94.1 sequence between *nl-1* and *pl-3* is consistent with data obtained from all *d-se* region mutants but one. All deficiencies that cover the *pl-2, nl-1* and *pl-3* groups, such as the Ae, Af, Be and Bf mutants, are deleted for p94.1. Similarly, mutants not deleted for *pl-2*, but deleted for the *nl-1* and *pl-3* groups, such as the Ac and Bd mutants, are deleted for the p94.1 sequence. Likewise, the Aj1 mutation, which "skips" the *pl-2, nl-1* and *pl-3* groups, and the Ab1 mutation, which "skips" the *pl-3* group, are not deleted for the p94.1 probe.

The only mutant not entirely consistent with the placement of p94.1 between *nl-1* and *pl-3* on the complementation map is the Bb2 *Df(dse)* mutant. Repeated densitometry analyses indicated that Bb2 is deleted for the p94.1 sequence, even though complementation analysis with Ac2 does not implicate a deficiency of pl-3. However, this mutant does give lethal combinations with Aa1 and with Ae1, which is in keeping with the proposed placement of p94.1. The complex results of the complementation analyses may indicate the presence of a small rearrangement.

The map position of the p0.7, p0.3 and pR1.3 probes between (*d, op*) and *nl-2* is consistent with all mutants analyzed (Figure 7). As expected, all *Df(dse)* deficiencies, which would be expected to delete the DNA between *d* and *se*, also delete the p0.3 sequence (Table 1). Mutants Ac1, Ac2 and Ae1, which are deficient for *nl-2*, are also deleted for p0.3. Moreover, the presence of the p0.3 sequence in the Db1 $se^{l}$ chromosome, which carries a deficiency that includes *nl-2* and extends distally past *se*, strongly suggests that p0.3 and its associated 45 kb of genomic DNA lie proximal to *nl-2* between (*d, op*) and *nl-2*.

The p94.1 and p0.3 probes can be used to discriminate among members of a single complementation group. For example, $d^{pl}$ mutant Aa1 carries two copies of p94.1, mutant Aa3 has one copy and mutant Aa2 carries the deletion breakpoint fusion fragment (ΔfAa2) from which the p94.1 probe was derived (Table 1). Likewise, mutants Bc1 and Bc2 can be distinguished using probe

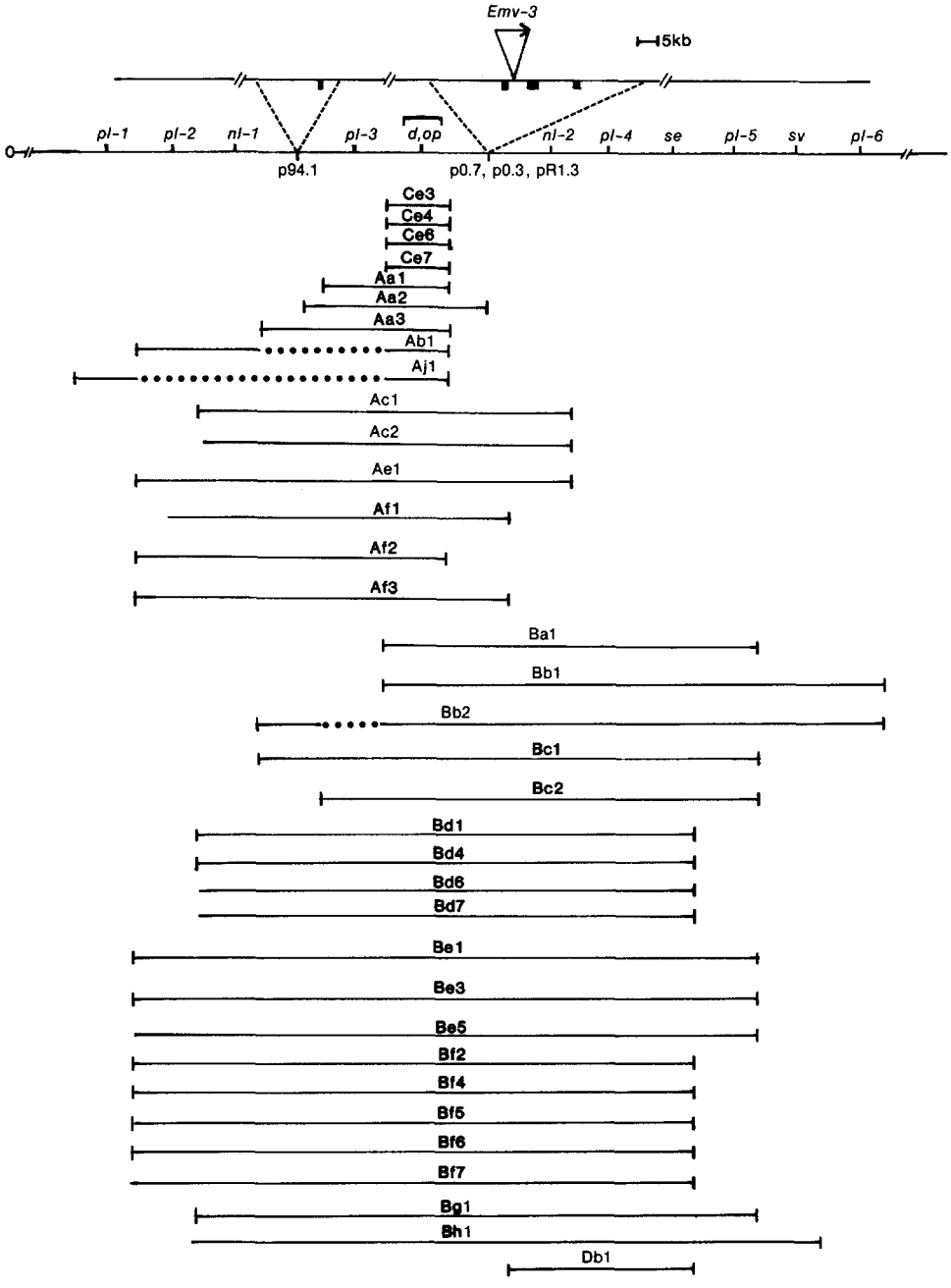


FIGURE 7.—Correlation of the *d-se* region physical and complementation maps. The placement of cloned probes, with their associated regions of DNA, onto the complementation map is indicated. The solid boxes on the physical map (top line) correspond to the probe sequences p94.1, p0.7, p0.3 and pR1.3, respectively, from left to right. The 5′ → 3′ direction of transcription of *Emv-3* is shown. Horizontal bars represent deficiencies, now aligned to demonstrate their extent with respect to both functional units and DNA markers. The proximal extent of the Ac2, Bd6, Bd7, Be5 and Bh1 deletions has not yet been determined precisely, and therefore is not indicated. These mutations have been assigned to specific complementation groups on the basis of available data. (See legend of Figure 1 for site designations.) Genetic distances (recombination frequencies): *d-se*, 0.16 cM; *se-sv*, 2 cM. The *se*$^{l}$ mutations Da1, Dc1 and Dd1 (Table 1) were not analyzed with probe 94.1 and therefore are not included in the figure.

p94.1. Both Aa1 and Aa3 mutants are wild type in the 45-kb region surrounding *Emv-3* (Table 1; data not shown), whereas mutant Aa2 carries a deletion breakpoint within the p0.3 probe sequence (Figure 4). Mutants Af1 and Af3, but not Af2, are deleted for sequences hybridizing to p0.3.

## DISCUSSION

The incorporation of the old *dilute* ($d^v$) and *short-ear* (*se*) mutations into the murine specific-locus mutagenesis screen (RUSSELL 1951) not only has made it possible to measure spontaneous and mutagen-induced mutation rates at these loci but also has provided over 200 radiation-induced and chemically induced mutations that are invaluable for genetic analysis of the *d-se* region of mouse chromosome *9*. In fact, RUSSELL (1971) has demonstrated that this region can be dissected into many functional units responsible for the control of diverse developmental pathways. This functional dissection was accomplished by genetic complementation analyses employing these radiation-induced mutations.

Molecular cloning of the *Emv-3* ecotropic murine leukemia provirus that is intimately associated with $d^v$ (JENKINS *et al.* 1981; COPELAND, HUTCHISON and JENKINS 1983; HUTCHISON, COPELAND and JENKINS 1984) has provided direct access to the *d-se* region at the molecular level. We have extended the physical analysis of the *d-se* region by studying the genomic structure of wild-type chromosomes, as well as that of chromosomes carrying the $d^{op}$, $d^{pl}$, $se^l$ and *Df(dse)* classes of radiation-induced mutations described by RUSSELL (1971). Analysis of these mutants has enabled us to orient the physical map of the dilute region, as it stands to date, with the complementation map. Moreover, four cloned nonviral DNA sequences can now be mapped to intervals on the functional (complementation) map.

The entire analysis of the *d-se* complex described in this report relied on deletion mapping of several cloned probes with the different classes of *d-se* radiation-induced mutations. Many $d^{pl}$ mutants and all *Df(dse)* mutants tested did, in fact, delete sequences homologous to a hybridization probe, p0.3, that was located approximately 3-kb distal to the 3′ LTR of the *Emv-3* provirus. This result, in itself, was significant because this was the first direct physical proof that at least some of the *d-se* region radiation-induced mutations are, indeed, deletions. Many of these mutants have been assumed to be deletions because they were defective in more than one functional unit (RUSSELL 1971). The present physical data now substantiate this hypothesis.

Analysis of the $d^{pl}$ deficiency carried in mutant Aa2 was critical to the orientation of the *d-se* region's physical and complementation maps. The p0.3 probe appeared to recognize sequences immediately 3′ to a deletion that extended in the 5′ direction past the *Emv-3* integration site. Cloning of this deletion breakpoint fusion fragment, ΔfAa2, from Aa2 DNA, and comparison of the restriction map of this fusion fragment with that of the p0.3 sequence confirmed this hypothesis. A probe derived from the 5′ end of ΔfAa2, p94.1, was then hybridized to the panel of *d-se* region mutants, resulting in the placement of this sequence in the interval between the *nl-1* and *pl-3* functional units. The p0.3 probe, which detects the 3′ end of the ΔfAa2 fusion fragment,

could then be placed between the (*d, op*) and *nl-2* groups. These results were consistent with the *Emv-3* provirus being oriented with the 5′ end proximal and the 3′ end distal toward *se*.

The placement of the p94.1 sequence into the *nl-1—pl-3* interval has several important consequences. First, this probe can be used in new chromosomal walking experiments, thus facilitating the molecular cloning of this region. Second, since p94.1 maps 5′ to the deletion breakpoint of *Df* (*dse*) mutant Bc2, by identifying and cloning the Bc2 deletion breakpoint fusion fragment it should be possible to effect another chromosome "jump" into a region distal to *d* that is associated with an interesting neurological disorder, Snell's waltzer (*sv*). Third, the p94.1 probe lies amid several prenatal and neonatal lethal factors defined by complementation analysis. This probe, therefore, will provide an important step in the analysis of the molecular nature of genes that appear to be critical for development of the embryo or for survival of the neonate. The ability of both the p0.3 and p94.1 probes to distinguish among members of a single complementation group, as well as among members of closely related complementation groups, is particularly cogent in this context. Additional cloned probes, which more precisely define the extent of these deletions, will ultimately allow the determination of the smallest segment of DNA that must be deleted to produce a specific mutant phenotype. This information, coupled with the comparison of deficiencies from other complementation groups, should ultimately allow the exact molecular definition of the *d-se* region genes responsible for the dilute, short-ear, neurological and prenatal/neonatal lethality phenotypes.

Complementation analysis of the Ab1, Aj1, Bb2, Dc1 and Dd1 mutants suggested that they may result from complex rearrangements, rather than from simple deletions. For example, the $d^{pl}$ mutant Ab1 complements $d^{pl}$ mutants deleted for *pl-3*, but does not complement $d^{pl}$ mutants deleted for both *pl-2* and *pl-3*. Thus, it appears as if Ab1 carries two deficiencies, one spanning *pl-2* and *nl-1*, and the other spanning (*d, op*) (Figures 1 and 7). Hence, the Ab1 deficiency appears to "skip" *pl-3*. We have confirmed that Ab1 is, likewise, not deleted for p94.1, which maps between *nl-1* and *pl-3*. Similarly, the Aj1 deficiency, which is hypothesized to skip *pl-2* and *nl-1* in addition to *pl-3*, also carries the p94.1 sequence. Thus, the Ab1 mutant could carry two deficiencies or could represent a complex inversion/deletion event in which the segment of DNA that includes *pl-2*, *nl-1*, p94.1 and *pl-3* was inverted to give the order *pl-1—pl-3—p94.1—nl-1—pl-2—*(*d, op*), followed by deletion of *nl-1*, *pl-2* and (*d, op*). This inversion/deletion hypothesis would then predict that the p94.1 sequence would be distal to *pl-3* [between *pl-3* and (*d, op*)] in the Ab1 mutant. The same type of argument could be made for the Aj1 "skipping" mutant, as well as for the Bb2 mutant, the latter of which was shown to be deleted for p94.1 but not for *pl-3*. Continued experiments that will enable cloning of other deficiency breakpoint fusion fragments and examination of the genomic organization of these classes of mutants will determine if these types of rearrangements occur. They have earlier been invoked to explain genetic results for two "skipping" $se^{l}$-mutations (RUSSELL 1971).

Large numbers of dilute and short-ear mutations have also been identified by specific-locus screening following mutagenesis with a variety of chemical agents, especially ethylnitrosourea (ENU) (RUSSELL *et al.* 1979). There is evidence that ENU-induced lesions are much smaller than radiation-induced ones and that some may be point mutations (RUSSELL 1982; POPP *et al.* 1983). Consequently, analysis of the gross organization of the *d-se* complex in radiation-induced mutations can be followed by analysis of these chemically induced mutations at the molecular level. These types of experiments not only will yield a fine-structure map of some of the genes in this complex but also will provide an understanding of the exact molecular effects on the mammalian germline of this class of mutagens.

Despite an initial understanding of the physical organization of the *d-se* complex, the nature of the effect of the *Emv-3* provirus on the dilute phenotype remains unclear. Previous studies have indicated that *Emv-3* does not produce the dilute phenotype in $d^v/d^v$ mice by integrating within the coding region of the dilute gene (COPELAND, HUTCHISON and JENKINS 1983; HUTCHISON, COPELAND and JENKINS 1984). Particularly puzzling is the fact that five of eleven $d^{pl}$ mutants and four $d^{op}$ mutants analyzed have no detectable deletions, insertions or rearrangements within the 45 kb surrounding the *Emv-3* integration site; and yet $d^{pl}/d^v$ and $d^{op}/d^v$ animals have a dilute phenotype indistinguishable from that of $d^v/d^v$ mice. Several explanations could account for these observations. First, the nine mutants in question may carry deficiencies that are very small and are not detectable with the techniques currently employed. Second, the *Emv-3* provirus could be exerting its mutagenic effect at some distance away from the dilute gene. Based on our analysis of the *d-se* region mutants, we would predict that, if this were the case, the dilute gene would be located 5′ to *Emv-3*, at least 16 kb away. There is some precedent for this type of interaction in which one genetic element influences the expression of another gene at some distance away (ZACHAR and BINGHAM 1982; MODELELL, BENDER and MESELSON 1983). Third, the dilute gene may be very large. Accordingly, deletions may be present that do not include the 45-kb region surrounding *Emv-3*. Continued analysis of the genomic organization of the numerous *d-se* region mutants, combined with an elucidation of the nature of the RNA transcripts derived from both mutant and wild-type chromosomes, should eventually make it possible to delineate the mechanism(s) by which integration of the *Emv-3* provirus induced the dilute phenotype, as well as provide an understanding of how genes in this complex function during development of the mouse.

SWEET (1983) recently identified a new recessive gene in the mouse, unlinked to *dilute*, that can suppress the mutant phenotype of *d/d* animals. This mutation, designated *dilute-suppressor* (*dsu*), is the first and only recessive suppressor to be identified in mammals. *dsu* does not appear to suppress the dilute phenotype by catalyzing the excision of *Emv-3* (N. A. JENKINS and N. G. COPELAND, unpublished results). Furthermore, $d^l/d^l$ animals homozygous for *dsu* are suppressed for the dilute phenotype but still due of opisthotonous (H. SWEET, personal communication). Experiments are in progress to test the ef-

fects of *dsu* on the many chemically induced and radiation-induced *dse* region mutations. These experiments afford a unique opportunity to analyze in a mammalian species the potentially complex interactions that are inherent in suppressor systems.

We thank CLYDE S. MONTGOMERY (Oak Ridge National Laboratory) for expert technical assistance and LINDA BRUBAKER (NCI-Frederick Cancer Research Facility) for typing this manuscript.

This work was supported by Damon Runyon-Walter Winchell Postdoctoral Fellowship DRG-787 (E.M.R.), National Cancer Institute grants CA-38039 and CA-37283, American Cancer Society grant MV-124 and National Cancer Institute, DHHS, under contract NO1-CO-23909 with Litton Bionetics, Inc. (N.G.C., N.A.J.), and the Office of Health and Environmental Research, U.S. Department of Energy, under contract DE-ACO5-840R21400 with the Martin Marietta Energy Systems, Inc. (L.B.R.).

## LITERATURE CITED

BENTON, W. D. and R. W. DAVIS, 1977 Screening of recombinant clones by hybridization to single plaques *in situ*. Science **196:** 180–182.

COPELAND, N. G., K. W. HUTCHISON and N. A. JENKINS, 1983 Excision of the DBA ecotropic provirus in dilute coat-color revertants of mice occurs by homologous recombination involving the viral LTRs. Cell **33:** 379–387.

COPELAND, N. G., N. A. JENKINS and B. K. LEE, 1983 Association of the lethal yellow ($A^y$) coat-color mutation with an ecotropic murine leukemia virus genome. Proc. Natl. Acad. Sci. USA **80:** 247–249.

DEOL, M. S. and M. C. GREEN, 1966 Snell's waltzer, a new mutation affecting behavior and the inner ear in the mouse. Genet. Res. **8:** 339–345.

GATES, W. H., 1928 Linkage of the factors for short ear and density in the house mouse. Genetics **13:** 170–179.

GREEN, M. C., 1981 *Genetic Variants and Strains of the Laboratory Mouse*, p. 218, Edited by M. C. GREEN. Gustav Fischer Verlag, Stuttgart.

HUTCHISON, K. W., N. G. COPELAND and N. A. JENKINS, 1984 Dilute-coat-color locus of mice: nucleotide sequence analysis of the $d^{+2J}$ and $d^{+Ha}$ revertant alleles. Mol. Cell. Biol. **4:** 2899–2904.

JENKINS, N. A., N. G. COPELAND, B. A. TAYLOR and B. K. LEE, 1981 Dilute (*d*) coat-color mutation of DBA/2J mice is associated with the site of integration of an ecotropic MuLV genome. Nature **293:** 370–374.

JENKINS, N. A., N. G. COPELAND, B. A. TAYLOR and B. K. LEE, 1982 Organization, distribution, and stability of endogenous ecotropic murine leukemia virus DNA sequences in chromosomes of *Mus musculus*. J. Virol. **43:** 26–36.

LYNCH, C. J., 1921 Short ears, an autosomal mutation in the house mouse. Am. Nat. **55:** 421–426.

MARKERT, C. L. and W. K. SILVERS, 1956 The effects of genotype and cell environment on melanoblast differentiation in the house mouse. Genetics **41:** 429–450.

MODELELL, J., W. BENDER and M. MESELSON, 1983 *Drosophila melanogaster* mutations suppressible by suppressor of hairy-wing are insertions of a 7.3-kilobase element. Proc. Natl. Acad. Sci. USA **80:** 1678–1682.

POPP, R. A., E. G. BAILIFF, L. C. SKOW, F. M. JOHNSON and S. E. LEWIS, 1983 Analysis of a mouse $\alpha$-globin gene mutation induced by ethylnitrosourea. Genetics **105:** 157–167.

RUSSELL, L. B., 1971 Definition of functional units in a small chromosomal segment of the mouse

and its use in interpreting the nature of radiation-induced mutations. Mutat. Res. **11:** 107–123.

RUSSELL, L. B. and D. L. DEHAMER, 1973 Complementation analysis of *c*-locus lethals in the mouse. Genetics **74:** s236.

RUSSELL, L. B., C. S. MONTGOMERY and G. D. RAYMER, 1982 Analysis of the albino-locus region of the mouse: IV. Characterization of 34 deficiencies. Genetics **100:** 427–453.

RUSSELL, W. L., 1951 X-ray-induced mutations in mice. Cold Spring Harbor Symp. Quant. Biol. **16:** 327–336.

RUSSELL, W. L., 1982 Factors affecting mutagenicity of ethylnitrosourea in the mouse specific-locus test and their bearing on risk estimation. pp. 59–70. In: *Environmental Mutagens and Carcinogens*, Edited by T. SUGIMURA, S. KONDO and H. TAKEBE. University of Tokyo Press, Tokyo.

RUSSELL, W. L., E. M. KELLY, P. R. HUNSICKER, J. W. BANGHAM, S. C. MADDUX and E. L. PHIPPS, 1979 Specific-locus test shows ethylnitrosourea to be the most potent mutagen in the mouse. Proc. Natl. Acad. Sci. USA **76:** 5818–5819.

SEARLE, A. G., 1952 A lethal allele of dilute in the house mouse. Heredity **6:** 395–401.

SILVERS, W. K., 1979 Dilute and leaden, the *p*-locus, ruby-eye, and ruby-eye-2. pp. 83–90. In: *The Coat Colors of Mice*, Edited by W. K. SILVERS. Springer-Verlag, New York.

SWEET, H. O., 1983 Dilute suppressor, a new suppressor gene in the house mouse. J. Hered. **74:** 305–306.

ZACHAR, Z. and P. M. BINGHAM, 1982 Regulation of *white* locus expression: the structure of mutant alleles at the *white* locus of *Drosophila melanogaster*. Cell **30:** 529–541.

Communicating editor: R. E. GANSCHOW